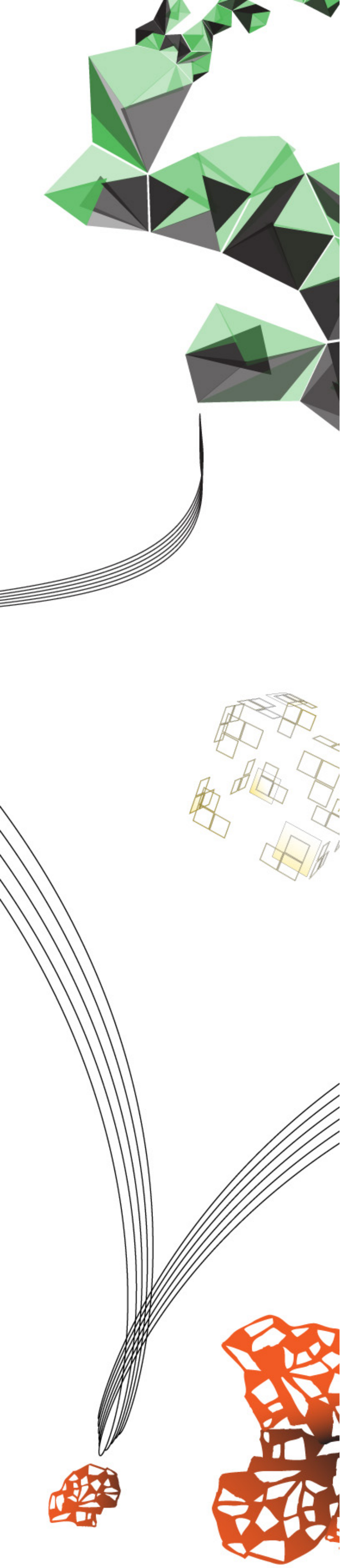

Bachelor assignment
Inorganic Membranes

In-situ characterization of thin layer polysulfone in water-toluene mixtures

Nicole Timmerhuis
s1226819
July 2015

Bachelor committee:
Prof. dr. J.G.E. Gardeniers (chairman)
Prof. dr. ir. N.E. Benes (graduation supervisor)
K. Tempelman, MSc (daily supervisor)
Dr. E.J. Kappert (daily supervisor)

UNIVERSITEIT TWENTE.

Abstract

Thin layer membranes are a kind of Solvent resistant nanofiltration (SRNF) membranes, which can be used to separate waste from waters on a molecular level. Thin film composite membranes consist of a polymeric top-layer on top of a porous support. Although SRNF membranes seem a promising technique, many challenges need to be overcome before the technique can be implemented on the large scale. One of the main challenges is the loss in stability. In many commercial membranes polysulfone (PSf) is used as support layer. However, this polymer dissolves in a liquid water/toluene mixture. The reason behind this is unclear. This report researches the behavior of PSf in water/toluene mixtures at different temperatures and toluene activities.

The results show that PSf dissolves at a temperature range of 18-30°C in a liquid water/toluene mixture. The PSf dissolves faster with increasing temperature. PSf reached a 250% swelling before dissolution in these measurements. The thin layer consists of 50% solvent and 50% polymer when a 100% swelling is reached. The normal dissolution mechanism is the most likely to occur during these measurements. This mechanism consists of two steps: solvent diffusion into the polymer and polymer chain disentangle into the solvent.

Secondly, the swelling behavior of the polysulfone is studied in toluene vapor. The swelling behavior is different in vapors compared to liquids. In toluene vapor the swelling degree is lower and other steps can be distinguished in the dynamics over time. According to Flory and Huggins, the activity decreases when the volume fraction of solvent in the polymer decreases. The activity of the toluene in the system most likely to be below 1 in the toluene vapor systems.

At last, toluene vapor is bubbled through water in the cell. Here, the activity seems lower with a lower toluene vapor flow at 18 °C. The toluene vapor refluxes in the top of the saturaters, which means that the toluene in the vapor flow is lower at 30 °C compared to 18 °C. This system has the opportunity to provide the information which is needed to distinguish the relation between the activity and toluene volume fractions, but improvements are needed to achieve this goal.

Acknowledgments

I would like to express my greatest gratitude to the people who have helped me during this bachelor assignment. Firstly, I would like to thank prof.dr. Louis Winnubst and his research group Inorganic Membranes for providing an opportunity to let me execute this bachelor assignment. Also I would like to thank dr.ir. Nieck Benes for his critical and very useful feedback and advises. I would like to give an extra gratitude of thanks to my daily supervisors MSc. Kristianne Tempelman and dr. Emiel Kappert, who guided my through this bachelor assignment and were always there to help me out. Last but not least I would like to thank my friends and family for their support throughout the project.

Contents

1 Introduction

In the oil and gas industry, water is a large waste product [1]. Around 3-10 barrels of waste water are generated for every barrel of oil produced. From all this waste water 95% can be reused for oil recovery. The remaining 5% is still a considerable amount of waste water. This waste water is contaminated with organic and inorganic compounds. The characteristics change per well of oil or gas, which makes it difficult to treat the waste water [2]. Chemical and biological methods were used before the use of membranes. These methods came with a lot of disadvantages like high costs of treatment, use of toxic chemicals, space for installation and secondary pollution [1]. Since the 21st century, membranes became a promising technique to replace the chemical and biological methods [1; 3].

Membranes can be used in several techniques to separate particles from a stream, such as microfiltration (MF), ultrafiltration (UF), nanofiltration (NF), and reverse osmosis (RO) [1]. All the techniques can be used for waste water treatment, in different stages of the process. In Table 1 can be seen which technique should be used to remove particles from a specific size. Nanofiltration and reverse osmosis are used for the final steps. Reverse osmosis is, for example, useful for the desalination of water. Nanofiltration is used for separation on a molecular level [4].

Table 1: Particle sizes which can be separated with different techniques [5].

Technique	Range (μm)
Microfiltration	1.5 – 0.1
Ultrafiltration	0.15 – 0.008
Nanofiltration	0.01 – 0.001
Reverse Osmosis	0.0015 – 0.0001

Solvent resistant nanofiltration (SRNF) membranes can be used to separate organic mixtures from their solutes (on the nanofiltration scale) [6]. Thin film composite membranes are a kind of SRNF membranes which consist of a polymeric top-layer on top of a porous support [7]. This is shown in Figure 1.

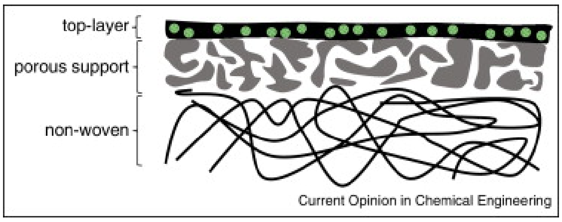

Figure 1: The different layers of a thin film composite membranes [6].

SRNF is still a young technique with a lot of advantages and disadvantages [4]. Advantages are that the separation does not involve a phase transition, the energy consumption is low, the membranes can be easily installed in a continuous process and it can be combined with existing processes [4]. However, it is not a proven technique yet [4]. The difficulty of the technique lies in the interactions between the solvent and solute, solvent and membrane, and solute and membrane. Every separation has specific molecular interactions which leads to specific membranes, which might not be available yet. The stability of the membranes can be seen as one of the main challenges in the development. The membranes are expected to be stable on the long term in a wide range of organic solvent at high temperature and pressure. At last, the boundary layer phenomena are of great importance, especially membrane fouling and concentration polarization are important issues. It can be seen that SRNF membranes offer a great opportunity for separating organic mixtures at a molecular level. However, lots of disadvantages come with this young technique which need to be solved before this technique can be implemented largely in the modern process industry [4].

Improving the stability of the SRNF membranes is one of the greatest challenges when it comes to implementing this technique on large scale in the process industry. The stability can be decreased by dissolved hydrocarbons in the waste water stream, which is the case for current desalination membranes (i.e. reverse osmosis membranes) [8]. Dissolvement of the polysulfone support layer is the reason for this decrease in stability. Polysulfone is stable in water and toluene, after a large swelling. However, the polysulfone is dissolving when water is saturated with toluene [8].

Yip [7] studied the morphology of the polysulfone support layer and polyester layer of thin-film composites. Self made membranes and current commercial membranes were compared to each other. The membrane performance of the thin film composites was not influenced after long exposure to saline water. It can be concluded that the polysulfone support layer is stable at different salt concentrations.

An example of unexpected behavior of a polymer in a solvent mixture is the behavior of poly-ϵ-caprolactone in water-acetone mixtures [9]. Water is a poor solvent and acetone is a good solvent for this polymer. The polymer chain behaves like predicted in the theoretical models when pure water or acetone is used. However, an abrupt change in trends is shown when a mixture of acetone and water is used. The acetone molecules are clustering together by forming hydrogen bonds. The clustering of acetone molecules has a great influence on the polymer structural and diffusion properties of the mixture [9].

The activity of water in polysulfone membranes is described by Schult [10]. Water is rare because it can form hydrogen bonds with itself and the polymer. The formation of water clusters is shown in Figure 2. The solubility in water is strongly dependent on the frequency of hydrogen bonding possibilities of the polymer. The water permeability is correlated to the free volume of the polymer but an overriding factor can be a favorable water-polymer interaction [10]. Water clustering can be identified by analyzing the activity and water diffusion coefficient [10]. The activity gives an indication of how much water is present in the mixture and the diffusion coefficient shows how fast water is diffusing into the polymer. Increasing activity with a decrease in diffusion coefficient, suggest water clustering.

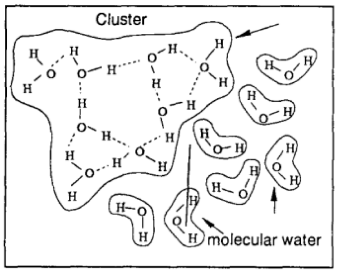

Figure 2: Formation of water clusters through hydrogen bonding [11].

The affinity between polysulfone and water is low, resulting in a low amount of swelling of the polysulfone film [8]. The thin layer swells excessively with toluene and dissolves in a mixture of water saturated with toluene. The swelling behavior of polysulfone is studied for different temperatures and toluene activities in this report. Different theoretical aspects are described in Chapter 2. The experimental procedures can be found in Chapter 3. Chapter 4 consist of the results and discussion and the conclusions are described in Chapter 5.

2 Theory

2.1 Polysulfone

Polysulfone is an engineering thermoplastic [12]. Thermoplastics have excellent impact strength and thermal and dimensional stability. Polysulfone is a linear aromatic polymer as shown in Figure 3. The glass transition temperature is 190°C and it has chain flexibility due to the ether linkages [12]. The molecular weight of the monomer is 444.545 g/mole.

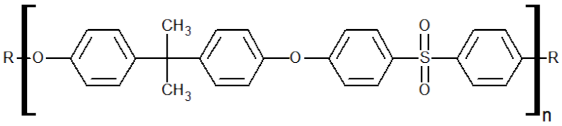

Figure 3: The structure of polysulfone [12].

2.2 Polymer dissolution

There are two main dissolution mechanisms which can occur with polymers in a solution [13]. Which mechanism will take place, is dependent of the solvent-polymer interactions. The first mechanism, the normal dissolution, takes place in two steps: solvent diffusion and chain disentanglement. The second mechanism consists of cracking the polymer into blocks which dissolve in the solvent.

2.2.1 Mechanism I: Normal dissolution

The first step in the normal dissolution mechanism is the diffusion of the solvent into the polymer [13]. The second step is chain disentanglement where the macromolecules are transported from the surface into the solution. These two steps are schematically shown in Figure 4.

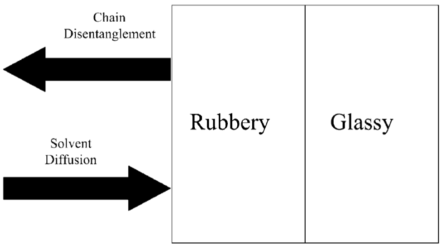

Figure 4: The two steps of polymer dissolution schematically shown. Step 1: the solvent diffuses into the polymer until a critical point is reached where no more solvent can diffuse into the polymer. Step 2: the polymer chains disentangle into the solvent and dissolution occurs. [13].

Solvents can diffuse into the polymer, causing the polymer to swell. In general, there are three different types of diffusion mechanisms which can be classified [14]:

1. Case I - Fickian diffusion: The rate of diffusion is smaller than the rate of the relaxation process.

2. Case II: The rate of diffusion is larger than the rate of the relaxation process.
3. Non-Fickian (anomalous) diffusion: The rate of diffusion is comparable to the rate of the relaxation process.

Glassy polymers are not at equilibrium but relax towards it [15]. Non-Fickian diffusion is the most common type of diffusion in these kind of polymers. The solvent can only diffuse into the polymer when the uncrosslinked, amorphous, glassy polymer is in contact with a thermodynamically compatible solvent [13]. Sorption curves can be determined by Equation 1 [14].

$$\frac{M_t}{M_\infty} = Kt^\alpha \tag{1}$$

where M_t is the mass of the solvent at time t and M_∞ is mass of solvent sorbed at equilibrium. The type of diffusion can be derived from α [14]. For Fickian diffusion, $\alpha = 1/2$. For non-Fickian diffusion, $1/2 < \alpha < 1$. Case II diffusion takes place when $\alpha \geq 1$. In Eq. 1 is K a constant, which is different for every type of diffusion. For Case I, K is the diffusion coefficient and in Case II is K the velocity of an advancing front of penetrating diffusant. The diffusion coefficient is dependent on the temperature, the diffusion coefficient increases with increasing temperature [16].

Different layers within the polymer film can be observed upon diffusion of the solvent into the thin polymer layer[13]. Figure 5 shows the several layers which are formed in the thin polymer layer, which were schematically shown in Figure 4. The pure solvent diffuses into the polymer, forming four types of layers. Every glassy polymer has empty spaces between the polymer chains, a free volume. This is the infiltration layer which will be filled with solvent at first. A solid swollen layer is formed secondly. Here is the polymer still in a glassy state. In the gel layer is the polymer more in a rubbery like state. The liquid layer is mostly liquid, with some polymer. The chain disentanglement occurs in the liquid layer, where the macromolecules are transported into the solution.

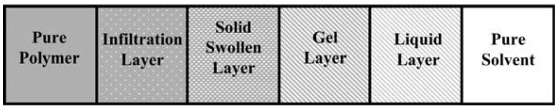

Figure 5: The different layers which are formed after diffusion of solvent into the thin layer [13]. The solvent diffuses into the polymer where two layers are formed. The polymer chains disentangle due to the diffusion of the solvent and dissolve into the solvent.

2.2.2 Mechanism II: Cracking of the polymer

No gel layer in the thin polymer layer is observed with the second proposed mechanism for polymer dissolution [13]. Small cracks in the polymer are observed with this mechanisms. The polymer matrix breaks and small blocks of polymer are erupted into the solution. This type of mechanism is only relevant below the glass transition temperature when no gel layer is observed in the polymer. The critical stress needed for these crackings to form is dependent on the molecular weight of the polymer. The cracking occurs below a critical molecular weight.

2.2.3 Dissolution variables

Polymer dissolution is dependent on several parameters [13]. The most important parameters are the polymer molecular weight, polymer structure, tacticity of the polymer and solvent type.

Firstly, the polymer molecular weight is an important parameter. The dissolution rate decreases with increasing polymer molecular weight. A higher degree of swelling is observed with higher molecular weights due to higher levels of chain disentanglement. Below a certain critical molecular weight, another dissolution mechanism will take place.

Secondly, the polymer structure is relevant for the mechanism of dissolution. An osmotic pressure stress is build up in the polymer layer. The rate of relieving this stress influences the type of dissolution mechanism. Normal dissolution takes place when the stress is relieved slowly. Otherwise, extensive cracking occurs in the polymer.

Thirdly, the tacticity of the polymer is relevant. Some types of tacticity can cause dissolution while another types can not. Which tacticity is relevant depends on the polymer.

Fourthly, different solvents have different influences on polymer the dissolution mechanism. The dissolution rate decreases with increasing solvent size due to that the solvents penetrate slower into the polymer when they are larger. Small non-solvent molecules can be added to a good solvent, which increases the dissolution rate.

2.3 Thermodynamic approach of polymers in solution

The thermodynamics of a polymer in solution can be described by the Flory-Huggins theory. In general, the energy of mixing can be described by the Gibbs free-energy of mixing, shown in Equation 2.

$$\Delta G_M = \Delta H_M - T\Delta S_M \tag{2}$$

ΔG_M is the free energy of mixing, ΔH_M is the enthalpy change on mixing, ΔS_M is the entropy change on mixing and T is the absolute temperature [13]. The mixing will occur spontaneously when ΔG_M is negative. For mixing systems there is a very small positive entropy change. Mixing is mostly dependent on the enthalpy change. According to Flory and Huggins the formation of the solution depends on the transfer of the polymer chain from a pure, perfectly ordered state to a state of disorder and the mixing process of the flexible chains with solvent molecules [17]. The entropy change on mixing is described in Equation 3.

$$\Delta S_M = S^M - S_1 - S_2 = -R(n_1 \ln\phi_1 + n_2 \ln\phi_2) \tag{3}$$

Where S^M is the ideal entropy of mixing, S_1 and S_2 are the entropy of the pure solvent and polymer respectively, R is the gas constant, n_1 and n_2 are the number of moles of the solvent and polymer respectively, and ϕ_1 and ϕ_2 are the volume fractions of the solvent and polymer [17].

The enthalpy of mixing can be described as a function of the interaction parameter, as shown in Equation 4. The interaction parameter, χ, is an important feature in the polymer solution theory which takes the energy of interdispersing polymer and solvent into account.

$$\Delta H_M = RT\chi_1 n_1\phi_2 \tag{4}$$

The Gibbs free energy can now be derived from Equation 2, 3 and 4.

$$\Delta G_M = RT[n_1 \ln \phi_1 + n_2 \ln \phi_2 + n_1 \phi_2 \chi_1] \tag{5}$$

More often, the equation above is expressed in terms of the partial molar Gibbs free energy of dilution.

$$\Delta G_M = RT[\ln(1-\phi_2) + (1-\frac{1}{r})\phi_2 + \chi_1 \phi_2^2] \tag{6}$$

Here, r is the degree of polymerization which is equal to 1 for the solvent. Equation 6 can be rewritten as a function of ϕ_1 and the activity, with $\Delta_r G = RT \ln a$, where $\Delta_r G$ is the Gibbs free energy of the reaction [16].

$$\ln a = \ln(\phi_1) + (1-\phi_1) + \chi_1(1-\phi_1)^2 \tag{7}$$

The Flory-Huggins theory has many limitations. The following assumptions are made: (1) the treatment assumed that the flexibility of the chain is unaltered on passing into the solution from the solid state; (2) interactions between the polymer and solvent which may lead to orientation of the solvent molecules near the polymer are neglected, this includes polar solutions; (3) the concentration and temperature dependency of the interaction parameter χ_1 is ignored [17]. There are several expansions of the Flory-Huggins theory due to these limitations. Hildebrand uses solubility parameters to determine the enthalpy of mixing (Eq. 8) [13].

$$\Delta H_M = V(\delta_1 - \delta_2)^2 \phi_1 \phi_2 \tag{8}$$

where δ_i $(i = 1, 2)$ is the solubility parameter of species *i*. The heat of mixing must be smaller then the entropic term for mixing to create a negative Gibbs free energy ($\Delta G_M \leq 0$). Therefore, the difference in solubility parameters must be small. This theory also does not take into account any specific interactions, like hydrogen bonds [13]. Hansen proposed that the solubility parameter is dependent on three types of interaction: non-polar interactions (D), dipole-dipole interactions (P) and hydrogen bonding (H). Hansen proposed the following dependence of the solubility parameter:

$$\delta_2 = \delta_D^2 + \delta_P^2 + \delta_H^2 \tag{9}$$

All the theories above are for two component systems. The Flory-Huggins theory can also be expanded to a three component system, with a polymer (3), solvent (2), and nonsolvent (1) [18]. Tompa extended the Gibbs free energy as following:

$$\frac{\Delta G_M}{RT} = \ln a = n_1 \ln \phi_1 + n_2 \ln \phi_2 + n_3 \ln \phi_3 + g_{12}(u_2) n_1 \phi_2 + \chi_{13} n_1 \phi_3 + \chi_{23} n_2 \phi_3 \tag{10}$$

In this equation is g_{12} used instead of χ_{12} because this interaction parameter is assumed to be concentration dependent. Therefore, g_{12} is expressed as $g_{12}(\phi_2) = \alpha + \beta / 1 - \gamma \phi_2$ where α, β and γ are empirical coefficients. In Eq. 10 g_{12} is a function of u_2, with $u_2 = \phi_2/(\phi_1 + \phi_2)$. The ternary interactions of the species are neglected in the equation above. An approximation of the interaction parameters can be calculated. The interaction parameter between the solvent (2) and polymer (3) can be calculated by the following equation:

$$\chi_{23} = \frac{v_2}{RT(\delta_2 - \delta_3)^2} + 0.34 \tag{11}$$

where v_2 is the molar volume of the solvent. This equation can only be used for nonpolar systems because the enthalpy contribution of specific interactions is not taken into account. The interaction parameter of the nonsolvent and polymer can be estimated by the Flory-Rehner equation:

$$\chi_{13} = -\frac{\ln(1-\phi_3)+\phi_3}{\phi_3^2} \tag{12}$$

2.4 Polymer-cosolvency phenomenon

In the section above it is assumed that a solvent and nonsolvent are used. The polymer swells when the Gibbs free energy for mixing is negative. It is possible that two nonsolvents together have such interactions that the solubility properties of the mixture are observed [19]. This is called the polymer-cosolvency phenomenon. The interactions between polar groups and formation of hydrogen bonds are important in these systems [20]. The Flory-Huggins theory, as discussed before, does not take these interaction into account so the theory can not be applied in these systems but extensions or alternatives of the theory must be applied. For example, Pouchly created a theoretical framework where hydrogen bonding is important [20]. This theory can only be applied when one of the two liquids interacts with the polymer while the other one stays inert.

2.5 Ellipsometry

Ellipsometry is a non-destructive optical technique that allows for very precise and accurate analysis of the optical properties, including film thickness and the refractive index of various thin film systems [21]. The change in polarization of reflected light is measured with ellipsometry. This is schematically shown in Figure 6. Figure 6a shows how the polarized light waves are transformed by the sample. Figure 6b shows the optical model of a typical used sample.

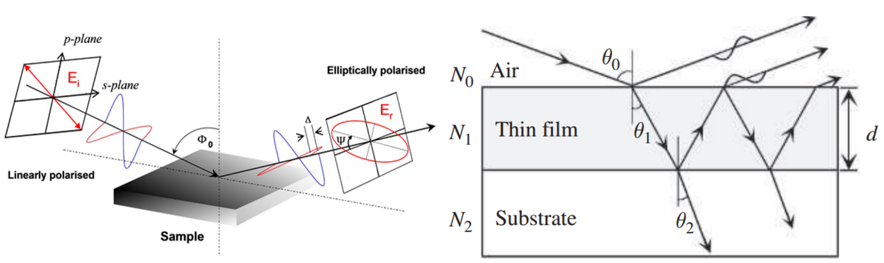

(a) *(b)*

Figure 6: [a]: Schematics of ellipsometry measurement principle [22]. [b]: Optical model consisting of an ambient/thin film/substrate structure [23].

A beam of light is reflected upon a sample under an angle of θ. By reflecting the beam, the light waves are polarized. The polarization of the light is measured with two parameters: Ψ and Δ. Ψ represents the angle determined from the amplitude ratio between p- and s-polarization, while Δ represents the phase difference of the two components [21]. These parameters are recorded for a set of wavelengths and are the basis for all the calculations. With several equations, the Ψ and Δ a model is created to fit the parameters to the properties of interest. The properties of interest are the film thickness and refractive index. The refractive index is calculated by the Cauchy dispersion:

$$n(\lambda) = A + \frac{B}{\lambda^2} + \frac{C}{\lambda^4} \tag{13}$$

Here, A, B and C are adjustable fitting Cauchy constants, n is the refractive index and λ is the wavelength. The accuracy of the fit can be derived from the MSE (Mean Squared Error). A lower MSE means that the fit is more accurate and reliable. The MSE value should be 0.5-2 for thin layers. For thick layers with much structure and/or oscillations in the data, a MSE of 10-20 is acceptable [24].

$$MSE = \sqrt{\frac{1}{2n-m}\sum_{i=1}^{n}[(N_{E_i} - N_{G_i})^2 + (C_{E_i} - C_{G_i})^2 + (S_{E_i} - S_{G_i})^2]} * 1000 \tag{14}$$

where n is the number of wavelengths, m is the number of fit parameters, and $N = cos(2\Psi)$, $C = sin(2\Psi)cos(\Delta)$ and $S = sin(2\Psi)sin(\Delta)$. The MSE as defined in Eq. 14 should actually be called the 'Root Mean Squared Error'.

Several parameters can be added to the fitting model to increase the quality of the fit and lower the MSE. Surface roughness is important because more light is scattered when the surface is rougher. With roughness (Figure 7a), the data is modeled with a Bruggeman Effective Medium Approximation mixing the top film with 50% void. The graded layer, as shown in Figure 7b, is another 'non-ideally' in the model. Here, the layer is subdivided in smaller sublayers. Each sublayer has its own optical properties, which are all slightly different. The film index 'n' is assumed to be a linear variation for the graded layer. [24]

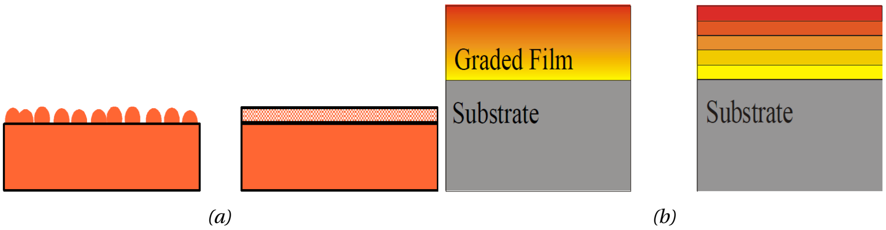

(a) (b)

Figure 7: [a]: An actual sample with a non-abrupt rough surface (left) and the optical model with the effective roughness layer (right). [b]: Graded layer as on a sample (left) and the approximation of the layer in the model (right) [24].

3 Experimental

The experimental procedures are described in this section. The total procedure consisted of three aspects: preparation of the thin film, ellipsometry measurements and result analysis.

3.1 Preparation of the thin film

Pure polysulfone was dissolved in cyclopentanone with 3wt% polymer. The clear, homogeneous solution was spin coated on a Silicon wafer using a Laurell WS-400B-6NPP-Lite Spinner spin coater in N_2 atmosphere to prevent influences of water. The wafer was cleaned with acetone before spinning. The spinning program consisted of 20 seconds on 600 rpm followed by 10 minutes on 800 rpm. In the first 20 seconds is the solution placed on the wafer with a pasteur pipette. The cyclopentanone was removed by placing the samples in an oven at 215°C for 8 h under N_2 with a temperature ramp of 5°C per minute. The samples were stored in a N_2 box before use.

3.2 Ellipsometry measurements

The software CompleteEASE was used to operate a Woollam α-SE ellipsometer. The sample was placed in a glass cell, which is made by the research group. The complete setup is shown in Figure 8.

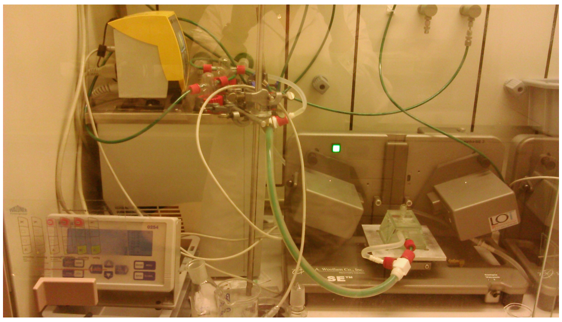

Figure 8: Setup of the Woollam α-SE. On the left is shown the temperature controlled water bath, with the saturaters. In front of the water bath stands a display where the settings can be changed from the mass flow controllers.

For the measurements the samples were cut in the desired sizes (between 1x1 cm and 2x2 cm). Six spots on the dry samples were measured in the cell before the in-situ measurements, to determine the thickness distribution on the silicon wafer. The average thickness and refractive index were calculated with the standard deviation. The ellipsometry measurements consisted measurements with a liquid water/toluene system at different temperatures, measurements with toluene vapor and a combination of toluene vapor and liquid water.

3.2.1 Swelling behavior of PSf in a liquid water/toluene system at different temperatures

In the liquid-liquid system was varied with the temperature. Distilled water was poured into the cell and left for around thirty minutes to equilibriate. The sample was carefully placed into the cell, after which the measurement could be started. After twenty minutes, the toluene was placed carefully on top of the water with a pasteur pipette. The thickness of the toluene was kept at around 5-10 mm during the measurement, so the water was saturated with toluene during the whole measurement. The setup for the liquid-liquid measurements is shown in Figure 9. The system was measured at 18 °C, 22 °C, 26 °C and 30 °C.

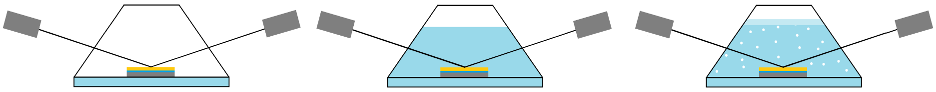

Figure 9: Setup of the temperature measurements. First, the dry samples were measured. Secondly, the water was poured into the cell and after thirty minutes was the sample placed into the cell. At last, the toluene was placed on top of the water.

3.2.2 Swelling behavior of PSf in toluene vapors

The gas flow measurements were done with two mass flow controllers. A N_2 flow went through two saturaters with toluene. The gas streams were led over the thin layer in the cell. This is schematically shown in Figure 10. The in-situ measurements lasted till the thin layer appeared to be stable. The thin layer was stable when the thickness did not change over the time. The different vapor flows were measured at 50, 80, 100, 150, 200 and 250 ml/min at a temperature of 18 °C.

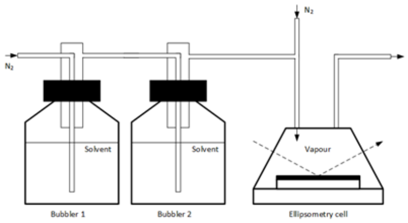

Figure 10: Schematic setup of the gas-system measurements. The nitrogenflow goes through two saturaters before it enters the cell.

Woollam cell

Figure 11 shows the Woollam cell with a volume of 500 μL. In this cell also a toluene vapor measurement was executed with a flow of 80 ml/min and 200 ml/min.

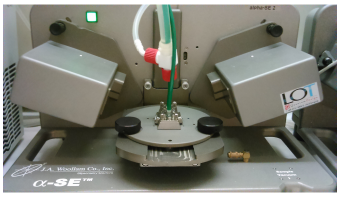

Figure 11: Setup of the Woollam cell for the toluene vapor measurements.

3.2.3 Swelling behavior of PSf in a gas-liquid system

The same mass flow controllers and saturaters were used as in the toluene vapor measurements. The dry samples were measured at first. Secondly, the cell was filled with distilled water. A saturated gas with toluene was led through the water in the cell, to let the water saturate with toluene. This was done for about twenty minutes before the samples was placed into the cell. The setup is schematically shown in Figure 12. In Table 2 are shown the measurement which were carried out with this system.

Table 2: The measurements which were carried out with the gas-liquid system.

#	Flow (ml/min)	Temperature (°C)
1	250	18
2	250	30
3	100	18

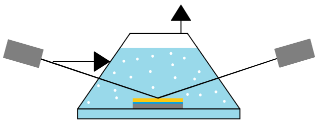

Figure 12: Setup of the gas-liquid system measurements. When the water is in the cell, a gas stream is led through the water of the cell.

3.2.4 PDMS measurements

A 5 wt% crosslinked PDMS (polydimethylsiloxane) in hexane was spincoated on a silicon wafer for one minute on 3000 rpm. The wafer was dried in the oven at 75°C for three hours. Two measurements were executed with the PDMS. The first measurement was a measurement with toluene vapor on 18 °C and a vapor flow of 80 ml/min. The second measurement was a measurement with water in the cell where toluene vapor was bubbled through at 30 °C and a vapor flow of 250 ml/min.

3.3 Analysis of the results

Figure 13: The different layers of the sample. The layer from top to bottom: surface roughness, thin PSf layer, native oxide, Si-wafer.

The sample has different layers which need to be taken into account while modeling the results. In Figure 13 is shown schematically the different layers of the sample. The Ψ and Δ data are fitted with a model of the CompleteEASE program. Therefore, the simplest model possible was used to fit the data. The model is shown in Appendix I. In the model, the Angle Offset and Delta Offset were fitted on the first data point and fixed on that value during the in-situ fit. The depolarization data was taken into account for all the in-situ measurements. The variables over time were Thickness, Graded Layer, A, B, C, and Thickness Non-Uniformity. The refractive index was calculated from the A, B and C with the Cauchy equation (Eq. 13).

Equation 15 was used to determine the swelling degree of the thin layer [17].

$$Swelling\% = \frac{t_{swollen} - t_{dry}}{t_{dry}} * 100\% \tag{15}$$

where $t_{swollen}$ is the thickness of the polymer during the measurement and t_{dry} is the thickness of the polymer before a solvent is used. For the liquid water/toluene systems the Thickness Pre-Fit was turned on to improve the fit. The gas-system measurements did not have a ambient > 1, so this parameter was turned off during the fit. For the other experiments is the ambient set on pure water with the assumption that the ambient was not influenced by the toluene. The swelling degree and refractive indices were plotted versus the time to compare different results with each other.

4 Results and discussion

This chapter is divided into three paragraphs. The influence of temperature at the swelling behavior of PSf is firstly studied in liquid water/toluene mixtures. The swelling behavior of PSf in toluene vapors is studied secondly. Finally, the swelling behavior of PSf is studied when toluene vapor is bubbled through water in the cell.

4.1 Swelling behavior of PSf in a liquid water/toluene mixture at different temperatures

In this section, the swelling behavior of PSf in a liquid water/toluene mixture is studied at different temperatures. It is already proven that PSf dissolves in a water/toluene mixture at 22 °C [8]. These measurements were carried out to distinguish the influence of the temperature.

The dry thickness of the thin layer was measured before the in-situ measurement. The average thickness can be seen in Table 3. The second sample has a higher average thickness and lower average refractive index. The lower average refractive index indicates that there is more free volume in the sample. Therefore, it is expected that this sample will swell slightly more compared to the first sample.

Table 3: Average thickness and refractive index per temperature of the dry samples before the temperature measurements.

#	Average thickness (nm)	Average refractive index (-)	T (°C)
1	192.98 ± 10.82	1.63205 ± 0.00724	18
2	213.26 ± 3.28	1.61591 ± 0.00724	18
3	193.65 ± 4.11	1.62845 ± 0.00077	18
4	195.57 ± 1.01	1.62133 ± 0.00387	22
5	196.16 ± 4.18	1.63870 ± 0.00448	26
6	176.87 ± 0.75	1.62797 ± 0.00046	30

The swelling degrees and refractive index are shown in Figure 14 of the in-situ measurements. The polysulfone starts to dissolve when the line reaches the highest point in the graph. After this point, the model was not applicable any more. All the measurements were ended when the Ψ and Δ showed the spectroscopic data of the silica wafer (shown in Appendix II). The wafers were also clean after the measurement as the spectroscopic data showed a typical Si-wafer graph.

All the measurements follow the same trend and reach almost the same swelling degree before dissolution. The swelling degree is around 250% in these measurements, while 40% swelling is reached in toluene vapor. A swelling degree of 100% means that the thickness is twice the thickness of the dry sample, the solvent provides for 50% of the total thickness. With a swelling degree above 100%, the fitting model has a high MSE. The polymer is dissolved according to the fitting model, when the polymer chains are completely disentangled and have the refractive index of the solvent.

The measurements at 18 °C show the most remarkable results. Three measurements were done under the same conditions. Figure 15 shows that three measurements with the same procedure can have three different results. In measurement (1), the PSf dissolves even faster than when the temperature is set at 22°C (shown in Figure 14). In measurement (2), the PSf dissolves after a long period of time. The last measurement appears to remain stable, although it was possible that the PSf dissolves when the measurement was done over a longer period of time.

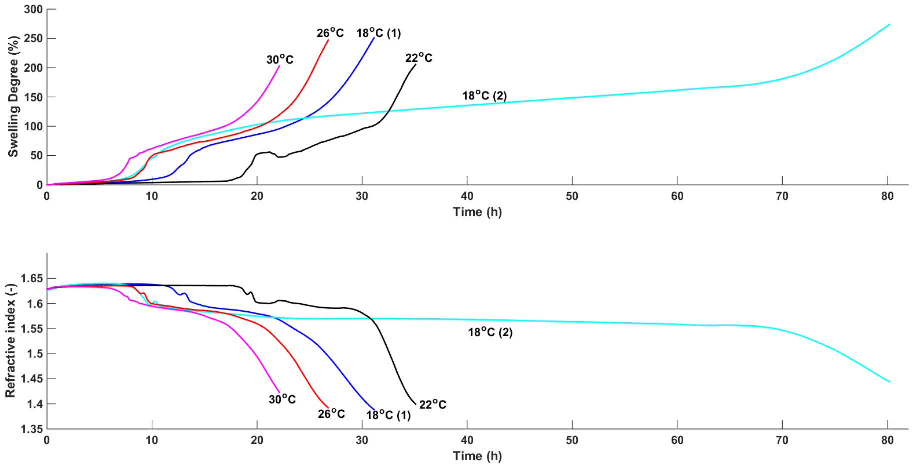

Figure 14: The swelling degrees versus time (above) and refractive index versus time (below) at different temperatures.

In Table 3 can be seen that the refractive index of the second sample is lower compared to the sample of the first measurement, which indicates a higher degree of free volume. The swelling degree is higher in the second measurement, which is due to the higher degree of free volume. One might think that with a higher degree of free volume, the PSf would dissolve faster. However, the results show the opposite because the PSf in the second measurement takes more time to dissolve. When the polysulfone has a swelling degree above 100%, the polysulfone is unstable in the solvent. One small disruption in the cell can cause the polymer to dissolve faster than expected. In the theory was stated that the dissolution rate decreases with increasing polymer molecular weight. Sample (2) had a higher thickness before the measurement and dissolved slower, compared to sample (1).

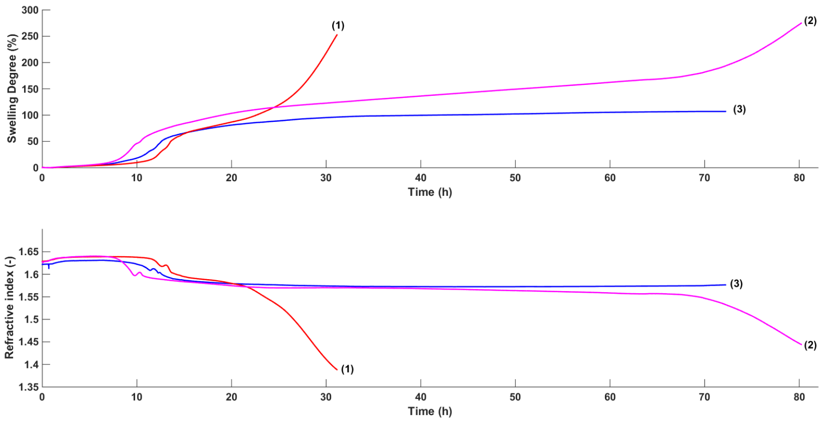

Figure 15: The swelling behavior of PSf in a liquid water/toluene mixture all at 18 °C. Three different measurements are carried out at the same conditions.

The PSf dissolves at all the measured temperatures in the liquid water/toluene mixture, which can be seen in Figure 14. The normal dissolution mechanism is most probable in this situation. With this mechanism, solvent diffuses first into the polymer forming five different layers in the thin polymer layer. Secondly, the polymer chains start to disentangle which is most likely to happen when the swelling is above 100%. The chain disentanglement leads eventually to the polymer dissolving into the solvent. The fitting model which is used includes thickness non-uniformity and a graded layer. With the cracking mechanism is no gel layer formed, so these fitting parameters would be less important. Also, with the cracking mechanism one would expect more abrupt changes in the swelling degree because the polymer breaks into small blocks which dissolve in the solvent. The normal dissolution mechanism seems most possible, due to the high swelling degree and no abrupt changes in the swelling degree in the results.

The PSf dissolves faster with higher temperatures. This is in agreement with the dissolving kinetics. When the temperature is higher, the diffusion of solvent into the polymer is faster. The first step of the normal dissolution mechanism occurs faster with a higher diffusion rate. The swelling degree is above 100%, which means that the thin layer consists of more solvent than polymer. This creates an unstable system. One small disruption in the cell can already change how fast the PSf is dissolving.

4.2 Swelling behavior of PSf in toluene vapors

The swelling behavior of PSf is studied under the influence of nitrogen flows saturated with toluene. The flow of the N_2 saturated with toluene is varied during these measurements. The swelling behavior of polysulfone is already known in liquid toluene and water, but not in toluene and water vapors. The goal of these experiments is to see if there is any change in swelling behavior of polysulfone in toluene vapor compared to liquid toluene and how these changes can be explained.

At first, the thickness and refractive index were measured of the dry sample. The average thickness of the dry samples are shown in Table 4. From this table, it can be seen that all the samples are between 190-205 nm with a rounded refractive index of 1.63.

Table 4: Average thickness and refractive index of the dry samples before the measurements. For which measurement the sample is used, can be seen in the last column.

#	Average thickness (nm)	Average refractive index (-)	Flow (ml/min)
1	193.56 ± 0.97	1.63029 ± 0.00201	50
2	197.87 ± 1.71	1.62804 ± 0.00192	80
3	193.00 ± 1.39	1.63240 ± 0.00292	100
4	192.98 ± 2.06	1.63069 ± 0.00472	150
5	203.40 ± 13.78	1.63029 ± 0.00198	200
6	197.44 ± 1.33	1.62460 ± 0.00400	250

Figure 16 shows the swelling behavior of PSf in liquid toluene [8]. Here, the swelling behavior can be divided in two sections. First are the overshoot dynamics where the swelling reaches a swelling degree around 85% in a short time. After these overshoot dynamics, the thin layer relaxes, which decreases the swelling. Here, the rate of diffusion is larger then the rate of relaxation, which indicates Case II diffusion.

First is looked at one measurement with a toluene vapor flow of 250 ml/min. Figure 17 shows the swelling degree and refractive index of this measurement. The swelling degree can be subdivided in

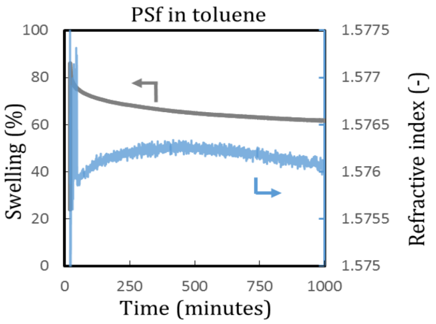

Figure 16: The swelling behavior of PSf in liquid toluene [8].

two parts and the refractive index in four parts. The first three parts of the refractive index are on the same timescale as the first part of the swelling degree.

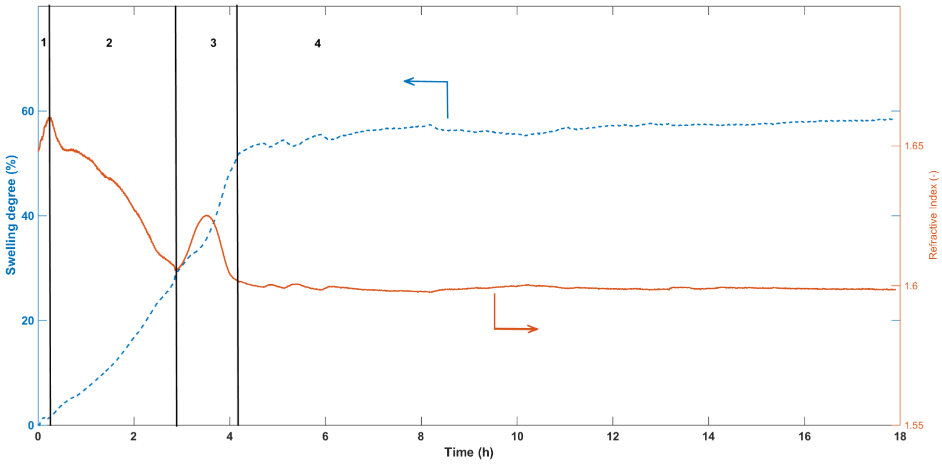

Figure 17: The different parts of the gasflow measurement which can be distinguished.

In the first part, the free volume of the polymer is filled with toluene. The density of the combined system increases, which increases the refractive index. After this increase, the polymer swells with the toluene vapor (part 2). The refractive index decreases during the swelling because the thin layer is now a mixture of polymer and toluene. Toluene has a refractive index of 1.496 [25].

The behavior of PSf in part 2 and 3 is both remarkable. The reasons behind this behavior is unknown. For part 2, it is possible that the process is not set yet. The toluene vapor is than not equally distributed over the cell, which means that the vapor does not reach the polymer thin layer equally. In part 3, the refractive index makes a sudden increase over a timescale of 40 minutes. After this increase, the refractive index decreases and stabilizes in part 4. The swelling degree also deviates in part 3. When the refractive index increases, the swelling degree differs from the trend it was following. It appears that the PSf collapses, which increases the refractive index and decreases the rate of increasing the swelling degree. After the small 'collapse', the toluene finds its way back to the PSf, causing a fast increase in swelling degree and decrease in refractive index. Part 4 is the stabilization of the polymer where the thickness and refractive index do not change over time.

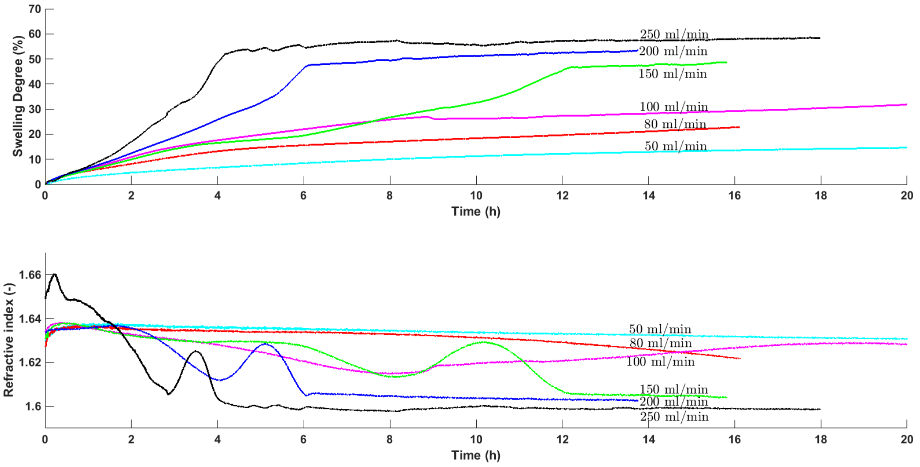

Figure 18: The behavior of PSf under the influence of toluene vapor at different flowrates. [Top panel]: Swelling degree versus time. [Bottom panel]: Refractive index versus time.

Figure 18 shows the swelling degree and refractive index of all the vapor measurements with different flows. The results per measurement are shown in Appendix II. As can be seen in Figure 18, the measurements at a flow of 150 ml/min and higher follow the same kind of curve in the refractive index and swelling degree. Below the flow of 150 ml/min, there is no clear distinction between different regimes. The maximum swelling degree which can be reached with toluene liquid is not reached at the lowest vapor flows.

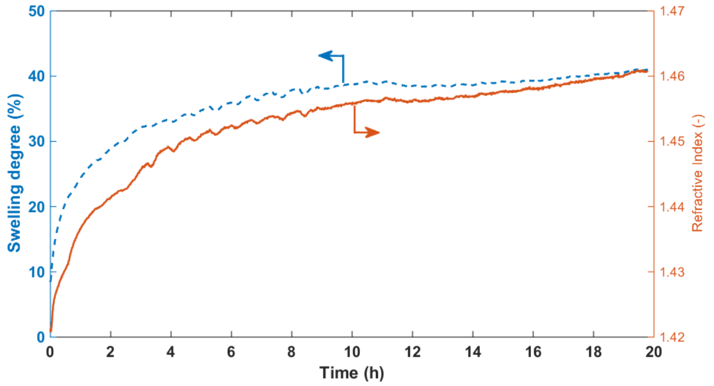

Figure 19: The swelling behavior of PDMS with toluene vapor at a flow of 80 ml/min

PDMS (polydimethylsiloxane) is used in the same toluene vapor setup to see if the toluene vapor reaches the sample. PDMS swelling equilibriates directly with toluene. The kinetics of the PDMS and PSf can be compared to each other with this experiment. One has to keep in mind that the swelling behavior of PDMS is different from the swelling behavior of PSf. PDMS swells 150% in liquid toluene.

The results are shown in Figure 19 where it can be seen that PDMS reaches a swelling degree of 40% after 20 h.

From this measurement, it might be possible that not enough toluene vapor reaches the sample to create a higher swelling degree. There is a million times more toluene brought to the cell than toluene which is needed to swell the PSf layer 100%. Here, it is assumed that toluene has the properties from a liquid in the layer and the layer swells exclusively from the toluene. Toluene has a molecular weight of 92.14 g/mole and the molecular weight of nitrogen is only 28.014 g/mole [25]. The cell is not ideally stirred, so it might be possible that the toluene vapor concentration builds up at the lowest point in the setup. It is possible that at the lowest flows, the flow is laminar. With a laminar flow, most of the toluene vapor never reaches the sample. At higher flows, the flow is more turbulent in the cell. When there is a turbulent flow, there is a better mixing of gas in the cell resulting in a more saturated toluene / nitrogen mixture in the cell. The residence time of a reactor is in general calculated as following: $\tau = V_{reactor}/\phi$ where τ is the residence time, $V_{reactor}$ the volume of the reactor and ϕ the flow. The residence time is calculated for every flow. The amounts of mole per minute were calculated with the Antoine equation and Ideal Gas law. The volume of the glass cell is 100 mL. The Woollam cell has a volume of 500μL, which is 140 times smaller than the glass cell.

Table 5: Flows and residence times per measurement

Flow (ml/min)	Flow (mmole/min)	τ (sec) glass cell	τ (sec) Woollam cell
50	0.0539	82.8	0.6
80	0.0863	51.8	0.375
100	0.1079	41.4	0.3
150	0.1618	27.6	0.2
200	0.2157	20.7	0.15
250	0.2696	16.6	0.1

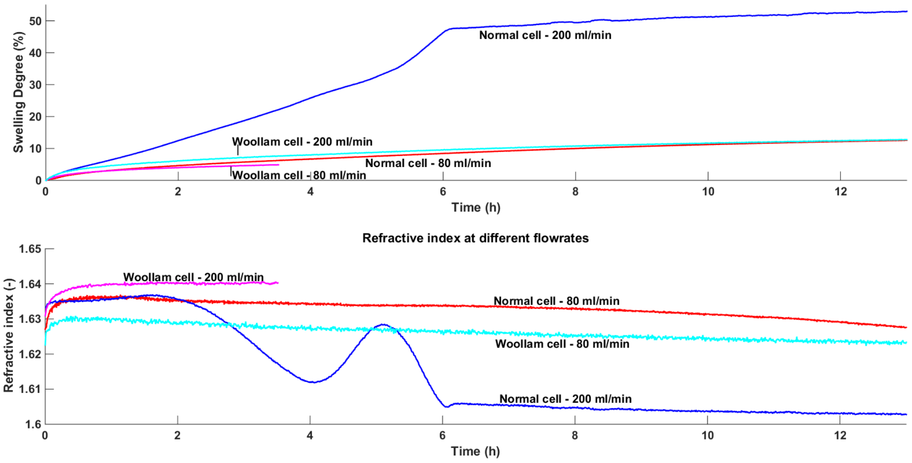

Figure 20: The swelling behavior of PSf in toluene vapor at different flow rates, the Woollam and glass cell compared to each other.

In the Woollam cell were two measurements done with a flow of 80 ml/min and 200 ml/min. The results can be seen in Figure 20. The swelling behavior in the Woollam cell is comparable to the swelling behavior in the glass cell with a flow of 80 ml/min. In the Woollam cell only small differences can be seen at different flows. These results show that the swelling behavior is not influenced by the flowrate in the Woollam cell.

It is clear that PSf and PDMS have different swelling behavior in vapors compared to liquids. Equilibrium is found at all flows, only at the lower flows it takes a longer period of time. Several explanations can be found for these differences. The activity might not be equal to 1 in the measurements. The sorption curve shows that when the activity is slightly below 1, there is a large difference in the amount of solvent diffused into the thin layer. The activity might not be equal to 1 because the flow is too low. When the flow is too low, there is a laminar flow of the vapor. The toluene vapor does not reach the thin layer with laminar flow. Schroeder described the differences of the swelling behavior in liquids and vapors as a paradox because thermodynamically seen, there should be no difference in the swelling behavior [26].

4.3 Swelling behavior of PSf in a gas-liquid system

The swelling behavior of PSf is studied when toluene vapor is bubbled through water in the cell. Several measurements are done with this system. The goal of these experiments is to create an experimental setup for measurements where the toluene activity in the water can be varied.

For these measurements are the average thickness and refractive index shown in Table 6. The average thickness of the first sample is a little bit higher compared to sample 2 and 3. Also, the first sample has the lowest free volume due to the highest refractive index.

Table 6: Average thickness and refractive index per temperature and flow of the dry samples before the activity measurements.

#	Average thickness (nm)	Average refractive index (-)	Flow (ml/min)	T (°C)
1	217.27 ± 8.10	1.63582 ± 0.00110	250	18
2	191.12 ± 2.45	1.61591 ± 0.00089	100	18
3	192.93 ± 2.62	1.62937 ± 0.00114	250	30
4 (PDMS)	430.05 ± 9.24	1.41276 ± 0.00233	250	30

In Figure 21, the results are shown of the measurements which are carried out at 250 ml/min. The PSf behaves quite different at 18°C and 30°C. At 18°C, it follows the same trend which one could see at the vapor measurements. The same swelling degree is reached when pure toluene vapor is led through the cell with and without water in the cell. The graphs show such similar trends that the water in the cell seem to have no influence on the swelling behavior, in this case. At 30 °C, there is almost no swelling over a long period of time for PSf as well as PDMS. Flory-Huggins have taught us that the solvent volume fraction in the polymer increases with increasing activity. The volume fraction of solvent in the polymer is lower at 30 °C compared to 18 °C, which indicates that there is a lower activity in the cell. The solubility increases with increasing temperature. However, the vapor consists of hydrophobic compounds and the water is hydrophilic. It might be possible that at higher temperatures, the degree mixing between the hydrophobic compounds in the vapor and hydrophilic liquid is lower and a higher degree of separation takes place. Therefore, the toluene does not reach the sample and leaves the cell before it can saturate the water. It is also possible that the toluene vapor already condensates in the saturaters due to the lower temperature in the top of the saturaters. The toluene vapor refluxes at the top of the saturaters until an equilibrium is reached. The amount of toluene in the vapor flow leaving the saturates is then lower at 30 °C versus 18 °C. Therefore, less toluene vapor enters the cell which creates a lower activity in the cell.

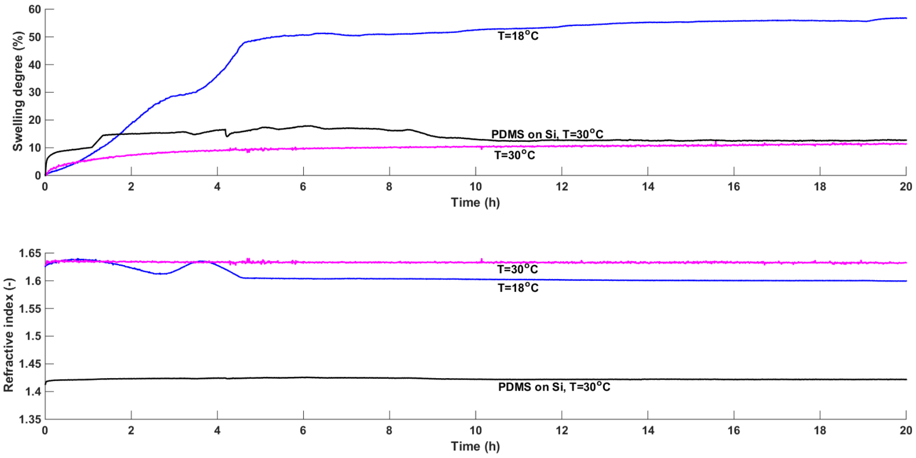

Figure 21: The swelling behavior of PSf and PDMS when toluene vapor is bubbled (with 250 ml/min) through water in the cell at different temperatures.

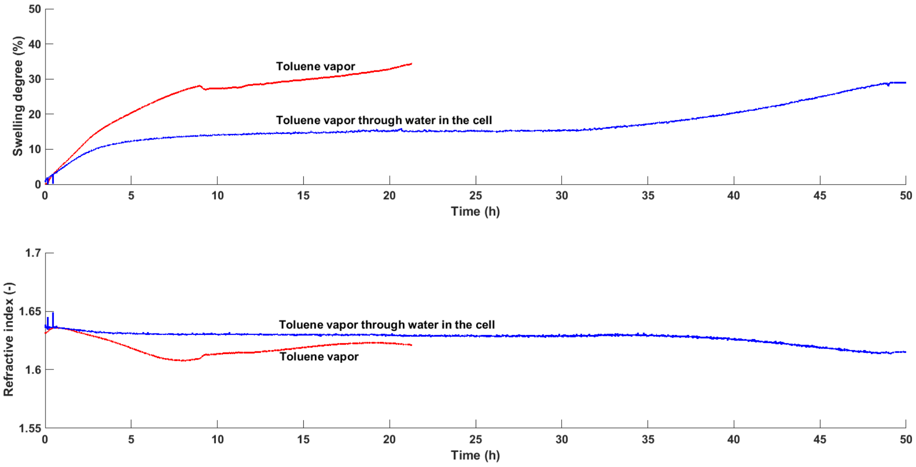

Figure 22: The swelling degrees versus time (above) and refractive index versus time (below) at 100 ml/min.

Figure 22 shows the results when the toluene vapor flow is 100 ml/min. These measurements are carried out at 18°C. For the pure gas measurement it is assumed that the toluene vapor has an activity of 1, this is lower for when the toluene vapor is bubbled through water in the cell. This can be seen in Figure 22, where the swelling degree is lower when toluene vapor is bubbled through the water in the cell compared to pure toluene vapor. The activity is than lower according to the Flory-Huggins theory. Although the activity is lower in the cell with water, the swelling behavior of the PSf is comparable to the swelling behavior in the liquid water/toluene mixture. It is remarkable that the PSf appears to be stable, but after 35 h starts to increase again. The swelling degree is still quite low, compared to the swelling degree in the liquid water/toluene mixtures. After the measurement, the sample was not uniform any more which indicates that some PSf was dissolved during the measurement.

The measurements as described in this paragraph showed some interesting results. Almost all the samples were not dissolved when the measurement was stopped. Only the measurement with a vapor flow of 100 ml/min at 18°C showed dynamics which were typical for the normal dissolution mechanism. Less toluene is carried to the cell when the flow rate is lower. This should decrease the activity of toluene in the cell. The swelling degree is lower with the flow of 100 ml/min compared to the vapor flow of 250 ml/min. At higher temperatures, the activity is lower in the cell due to the condense which is formed in the saturaters. The formation of condense ensures that the activity of the toluene vapor flow is below 1. With these measurement, there can be no conclusions made about the activity dependency of the solubility mechanism. More research needs to be done before a clear dependency can be distinguished.

5 Conclusion

The swelling behavior of polysulfone was studied with different parameters. A liquid water/toluene mixture is used to determine the influence of temperature. The results show that PSf dissolves at a temperature range of 18-30°C. The PSf dissolves faster with increasing temperature. PSf reached a 250% swelling before dissolution in these measurements. When a 100% swelling is reached, the thin layer consists of 50% solvent and 50% polymer. Above a swelling degree of 100%, the thin layer is unstable and small changes in the environment or sample can cause a fast or slow dissolution. The normal dissolution mechanism is the most likely to occur during these measurements. This mechanism consists of two steps: solvent diffusion into the polymer and polymer chain disentanglement. In the second step, the polymer is transported from the thin layer into the solvent. In the results can be seen that the solvent diffuses into the thin layer causing it to swell. The diffusion rate of the polymer increases after 100% swelling. The refractive index decreases below the refractive index of toluene. The polymer chains disentangle and, finally, are transported into the solvent.

Secondly, the swelling behavior of the polysulfone is studied in toluene vapors at different vapor flows. A swelling degree of 85% is reached in liquid toluene in a few minutes. After that, the polysulfone relaxes and stabilizes till a swelling degree of 70%. PSf shows different behavior in toluene vapors. A maximum swelling degree of 60% is reached after 4 h at a toluene vapor flow of 250 ml/min. Also, the dynamics are different in vapors compared to liquids. Overshoot dynamics and relaxation take place in liquid toluene. The measurement can be divided in four different parts for the toluene vapors: (1) the free volume is filled with toluene, (2) the process is finding its equilibrium, (3) the PSf collapses, which increases the refractive index and decreases the rate of swelling, (4) the thin layer stabilizes. These four parts can also be distinguished when the toluene vapor flow is 200 ml/min and 150 ml/min. Different swelling behavior is shown below a toluene vapor flow of 150 ml/min. Here, the swelling stays lower compared to the higher flows. The differences in swelling behavior can be explained by the Flory-Huggins theory, which states that a lower volume fraction of solvent in the polymer is reached when the activity is lower.

No dissolution is observed when toluene vapor is bubbled through water in the cell. Toluene vapor refluxes in the saturators causing the toluene vapor activity to decrease at 30 °C. The same swelling degree is reached when pure toluene vapor is led through the cell with and without water in the cell, at a flow rate of 250 ml/min and 18 °C. Not the same swelling degree is reached when there is water in the cell compared to the toluene vapor, when the toluene vapor flow is 100 ml/min. This indicates that the activity is decreases with a decreasing flow rate.

6 Recommendations

Several recommendations can be made for further research on this topic. The temperature range can be expanded to lower and higher temperatures till the PSf stops dissolving into the liquid water/toluene mixture. For example, one can measure first at 10 °C and 40 °C to see if these measurements follow the same trend which was shown in this report. Also, QCM can be added to the ellipsometry measurements to measure the weight differences over time. With QCM, a more precise moment can be determined when the polysulfone is dissolved.

The measurements with the toluene vapors can also be improved by duplicate measurements. The measurements can be carried out over a longer period of time to see if they reach the swelling degree of 60 % for the toluene vapor flows below 150 ml/min. Also, the flow and composition of the flow at the end of the cell should be measured to see if the toluene vapor builds up in the cell or not. The Woollam cell can be used when the flow is not supposed to have an influence on the measurements. At last, the flows of 300 ml/min and 350 ml/min can be measured to see if the process can reach its equilibrium faster.

The measurements can be improved when toluene vapor is bubbled through water in the cell. In general, the measurements at 18 °C should be done over a longer period of time to see if dissolution occurs in this system. Secondly, the outgoing vapor composition can be determined with GC/MS. A mass balance can be made with the known outgoing vapor composition from which the activity of toluene in the cell can be determined. The temperature in the cell was not measured during the in-situ measurement. Therefore, it is not known if the temperature was stable in the cell. This can be improved by placing a temperature sensor in the cell during the measurement. Also, the water level was decreasing during the measurement. When the water level is too low, the vapor flow goes over the water to the outlet instead of through the water. Water should be added carefully during the measurements so it does not influences the stationary state of the cell. The Woollam cell can be used so the flow does not has an influence on the activity. One has to keep in mind that the Woollam cell is not temperature controlled yet.

7 List of symbols

Table 7: List of symbols.

α	constant
δ	solubility parameter
Δ	phase difference
θ	angle
λ	wavelength
τ	residence time
ϕ	volume fraction
χ	interaction parameter
ψ	angle from the amplitude ratio
a	activity
A, B, C	adjustable Cauchy constants
G	Gibbs free energy
H	enthalpy
K	constant
M_t	mass of the solvent sorbed at time t
M_∞	mass of the solvent sorbed at equilibrium
n	number of moles
n	refractive index
r	degree of polymerization
R	gas constant
S	entropy
t	time
T	temperature
v	molar volume
V	volume

8 Bibliography

[1] Ahmadun FakhruŠl-Razi, Alireza Pendashteh, Luqman Chuah Abdullah, Dayang Radiah Awang Biak, Sayed Siavash Madaeni, and Zurina Zainal Abidin. Review of technologies for oil and gas produced water treatment. *Journal of Hazardous Materials*, 170(2):530–551, 2009.

[2] Mehmet Çakmakce, Necati Kayaalp, and Ismail Koyuncu. Desalination of produced water from oil production fields by membrane processes. *Desalination*, 222(1):176–186, 2008.

[3] SS Madaeni and L Bakhtiari. Thermodynamic-based predictions of membrane morphology in water/dimethylsulfoxide/polyethersulfone systems. *Polymer*, 53(20):4481–4488, 2012.

[4] Pieter Vandezande, Lieven E. M. Gevers, and Ivo F. J. Vankelecom. Solvent resistant nanofiltration: separating on a molecular level. *Chem. Soc. Rev.*, 37:365–405, 2008. doi: 10.1039/B610848M. URL `http://dx.doi.org/10.1039/B610848M`.

[5] h_2o distributors - particle size chart: Removal range by filtration. URL `http://www.h2odistributors.com/chart-particle-sizes.asp`.

[6] Sanne Hermans, Hanne Mariën, Cedric Van Goethem, and Ivo FJ Vankelecom. Recent developments in thin film (nano)composite membranes for solvent resistant nanofiltration. *Current Opinion in Chemical Engineering*, 8(0):45 – 54, 2015. ISSN 2211-3398. doi: http://dx.doi.org/10.1016/j.coche.2015.01.009. URL `http://www.sciencedirect.com/science/article/pii/S2211339815000106`.

[7] Ngai Yin Yip, Alberto Tiraferri, William A. Phillip, Jessica D. Schiffman, and Menachem Elimelech. High performance thin-film composite forward osmosis membrane. *Environmental Science & Technology*, 44(10):3812–3818, 2010. doi: true. URL `http://dx.doi.org/10.1021/es1002555`. PMID: 20408540.

[8] M.A. Van Kuppevelt. The effect of dissolved hydrocarbons on the stability of reverse osmosis membranes. Master's thesis, University of Twente, 2015.

[9] Nicodemo Di Pasquale, Daniele Luca Marchisio, Antonello Alessandro Barresi, and Paola Carbone. Solvent structuring and its effect on the polymer structure and processability: The case of waterâĂŞacetone poly-Îţ-caprolactone mixtures. *The Journal of Physical Chemistry B*, 118(46): 13258–13267, 2014. doi: 10.1021/jp505348t. URL `http://dx.doi.org/10.1021/jp505348t`. PMID: 25383480.

[10] K.A. Schult and D.R. Paul. Water sorption and transport in a series of polysulfones. *Journal of Polymer Science, Part B: Polymer Physics*, 34(16):2805–2817, 1996. URL `http://www.scopus.com/inward/record.url?eid=2-s2.0-0030286961&partnerID=40&md5=ab89520b5cef0c969d203a64184b52dd`. cited By 60.

[11] QT Nguyen, E Favre, ZH Ping, and J Neel. Clustering of solvents in membranes and its influence on membrane transport properties. *Journal of membrane science*, 113(1):137–150, 1996.

[12] R.O. Ebewele. *Polymer Science and Technology*. CRC Press LLC, 2000.

[13] B.A. Miller-Chou and J.L. Koenig. A review of polymer dissolution. *Progress in Polymer Science*, 28: 1223–1270, 2003. doi: 10.1016/S0079-6700(03)00045-5.

[14] J. Stastna and D. De Kee. *Transport Properties in Polymers*. Technomic Publishing Company, Inc., 1995.

[15] P. Neogi. *Diffusion in Polymers.* Marcel Dekker, Inc., 1996.

[16] Peter Atkins and Julio de Paula. *Physical Chemistry.* W.H. Freeman and Company, 9th edition edition, 2010. doi: 978-0-19-954337-3.

[17] John Mackenzie Grant Cowie and Valeria Arrighi. *Polymers: chemistry and physics of modern materials.* CRC Press, 2007.

[18] Li Xu and Feng Qiu. Simultaneous determination of three flory–huggins interaction parameters in polymer/solvent/nonsolvent systems by viscosity and cloud point measurements. *Polymer*, 55 (26):6795–6802, 2014.

[19] Yasuhiro Miyako, Yinyan Zhao, Kazuo Takeshima, Takahiro Kataoka, Tetsurou Handa, and Rodolfo Pinal. Solubility of hydrophobic compounds in water–cosolvent mixtures: relation of solubility with water–cosolvent interactions. *Journal of pharmaceutical sciences*, 99(1):293–302, 2010.

[20] Arturo Horta, Deodato Radic, and Ligia Gargallo. Association equilibria theory of preferential adsorption in systems with solvent-solvent and solvent-polymer interactions. *Macromolecules*, 22(11):4267–4272, 1989. doi: 10.1021/ma00201a022. URL `http://dx.doi.org/10.1021/ma00201a022`.

[21] Wojciech Ogieglo. *In-situ spectroscopic ellipsometry for studies of thin films and membranes.* Universiteit Twente, 2014.

[22] Surface and interface physics, ellipsometry. URL `https://www.tcd.ie/Physics/Surfaces/ellipsometry2.php`.

[23] Hiroyuki Fujiwara. *Spectroscopic ellipsometry: principles and applications.* John Wiley & Sons, 2007.

[24] Inc. J.A. Woollam Co. *CompleteEASE Data Analysis Manual*, 2011.

[25] Msds toluene. URL `https://www.sigmaaldrich.com`.

[26] Cécile Vallieres, Dirk Winkelmann, Denis Roizard, Eric Favre, Philip Scharfer, and Matthias Kind. On schroeder's paradox. *Journal of membrane science*, 278(1):357–364, 2006.

Appendices

Appendix I: Fitting model of CompleteEASE

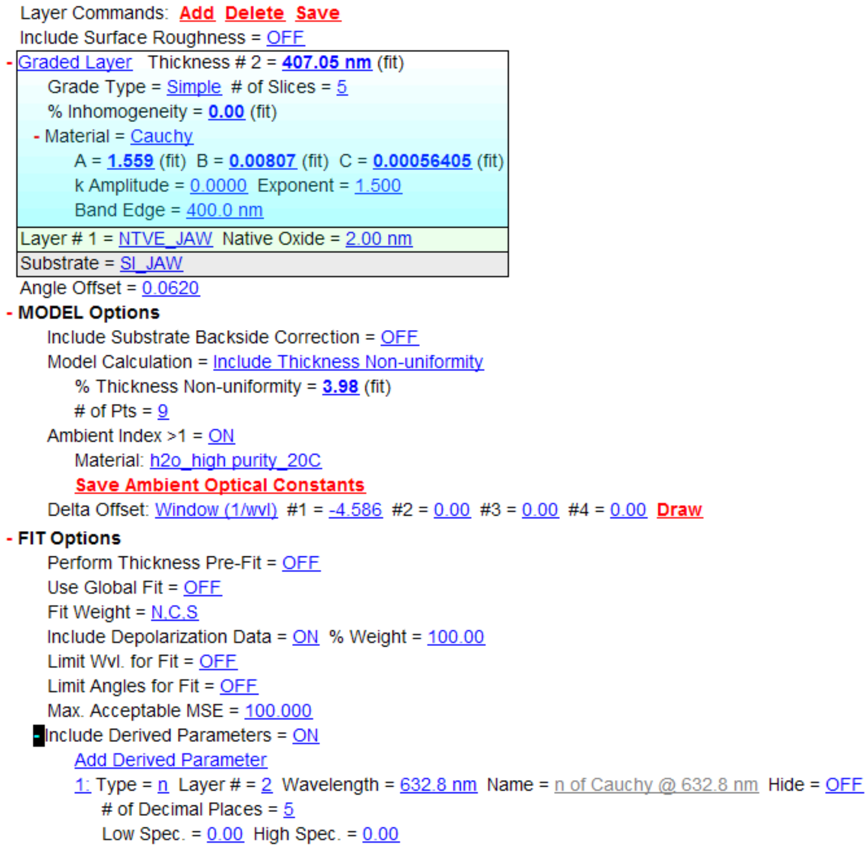

```
  Layer Commands:  Add  Delete  Save
  Include Surface Roughness = OFF
- Graded Layer   Thickness # 2 = 407.05 nm (fit)
      Grade Type = Simple  # of Slices = 5
      % Inhomogeneity = 0.00 (fit)
    - Material = Cauchy
          A = 1.559 (fit)  B = 0.00807 (fit)  C = 0.00056405 (fit)
          k Amplitude = 0.0000  Exponent = 1.500
          Band Edge = 400.0 nm
  Layer # 1 = NTVE_JAW  Native Oxide = 2.00 nm
  Substrate = SI_JAW
  Angle Offset = 0.0620
- MODEL Options
      Include Substrate Backside Correction = OFF
      Model Calculation = Include Thickness Non-uniformity
          % Thickness Non-uniformity = 3.98 (fit)
          # of Pts = 9
      Ambient Index >1 = ON
          Material: h2o_high purity_20C
          Save Ambient Optical Constants
      Delta Offset: Window (1/wvl)  #1 = -4.586  #2 = 0.00  #3 = 0.00  #4 = 0.00  Draw
- FIT Options
      Perform Thickness Pre-Fit = OFF
      Use Global Fit = OFF
      Fit Weight = N.C.S
      Include Depolarization Data = ON  % Weight = 100.00
      Limit Wvl. for Fit = OFF
      Limit Angles for Fit = OFF
      Max. Acceptable MSE = 100.000
    - Include Derived Parameters = ON
          Add Derived Parameter
          1: Type = n  Layer # = 2  Wavelength = 632.8 nm  Name = n of Cauchy @ 632.8 nm  Hide = OFF
              # of Decimal Places = 5
              Low Spec. = 0.00  High Spec. = 0.00
```

Figure 23: The model which is used to fit Ψ and Δ. The Angle Offset and Delta Offset were set at the beginning of the measurement. The Ambient index >1 was turned off with the vapor experiements. The Perform Thickness Pre-Fit is turned on when the raw data at the end showed the data for a Si-wafer.

Appendix II: Raw data of measurements

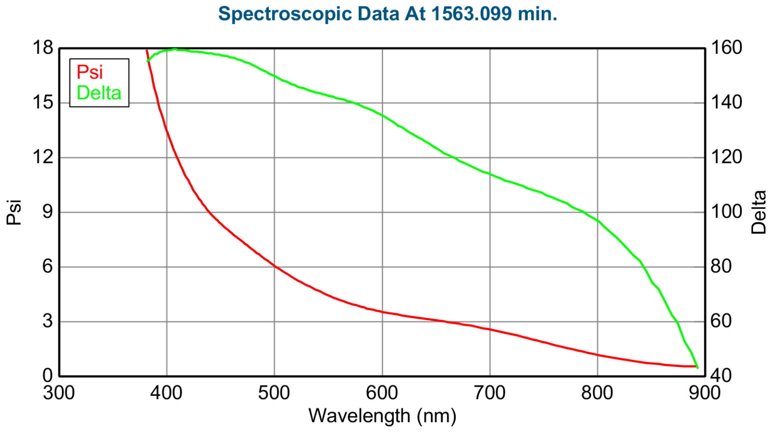

Figure 24: The spectroscopic data (Ψ and Δ) which is typical for a clean Si-wafer.

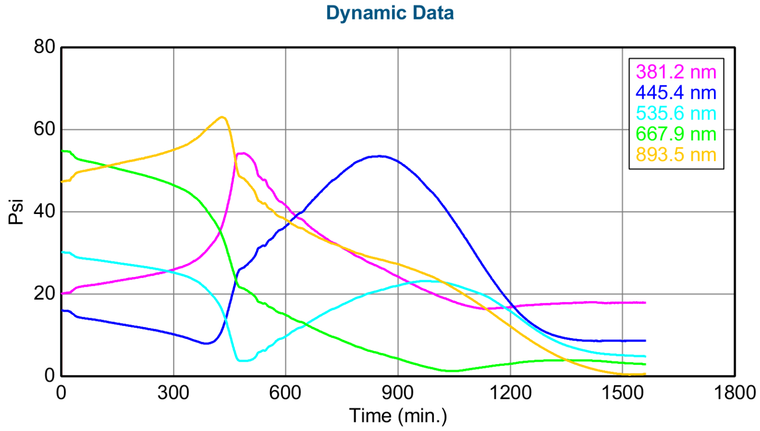

Figure 25: The dynamic data (Ψ) of the measurement with a liquid water/toluene mixture at 30°C.

Appendix III: Flow measurement results

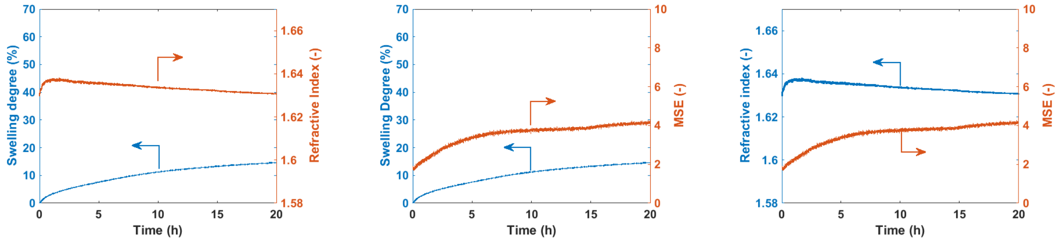

Figure 26: Flow = 50 ml/min

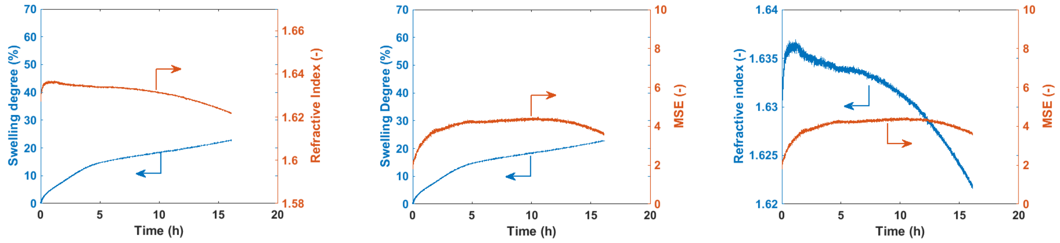

Figure 27: Flow = 80 ml/min

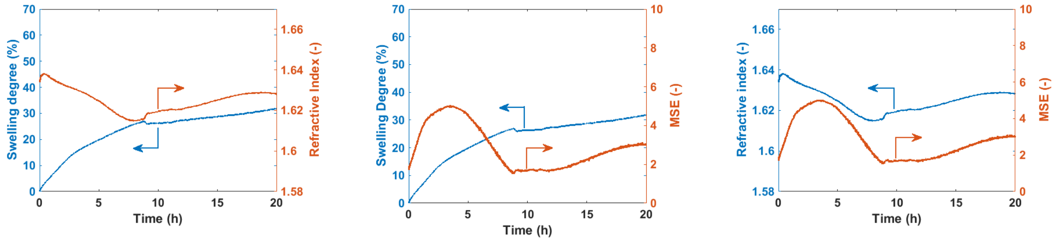

Figure 28: Flow = 100 ml/min

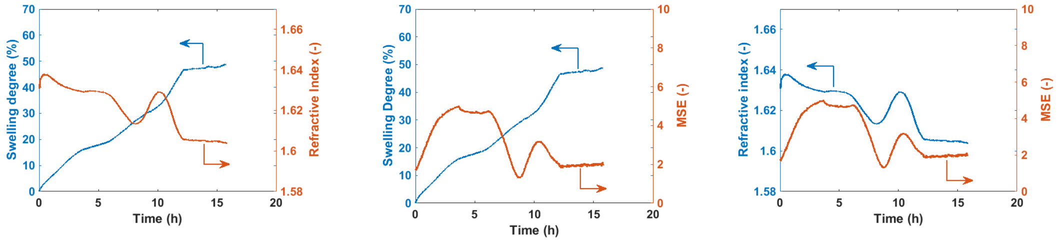

Figure 29: Flow = 150 ml/min

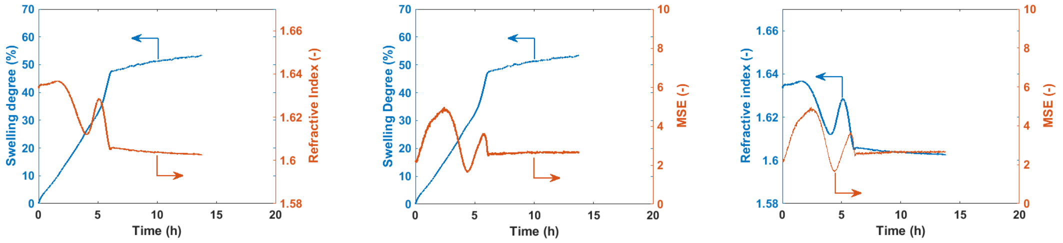

Figure 30: Flow = 200 ml/min

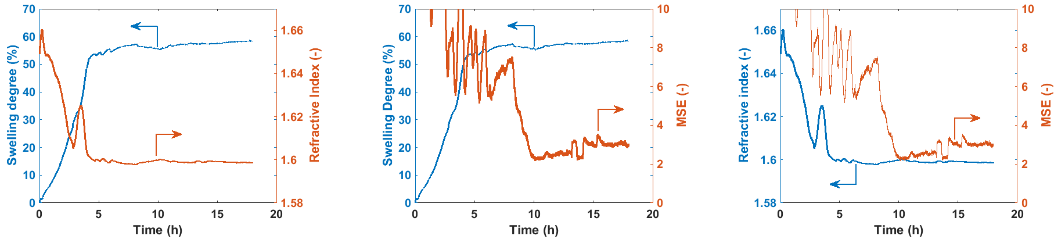

Figure 31: Flow = 250 ml/min